



Published in final edited form as:

Pain. 2020 March ; 161(3): 630–640. doi:10.1097/j.pain.0000000000001753.

Brain signatures of threat-safety discrimination in adolescent chronic pain

Lauren C. Heathcote^{1,*}, Inge Timmers¹, Corey A Kronman¹, Farah Mahmud², J. Maya Hernandez¹, Jason Bentley³, Andrew M Youssef², Daniel S. Pine⁴, David Borsook², Laura E. Simons¹

¹Department of Anesthesiology, Perioperative, and Pain Medicine, Stanford University School of Medicine, 1070 Arastradero Road, Palo Alto, CA 94304

²Center for Pain and the Brain, Massachusetts General Hospital, Boston Children's Hospital, and McLean Hospital, Harvard Medical School, 300 Longwood Avenue, Boston, MA 02115

³Quantitative Science Unit, Stanford University, 1070 Arastradero Road, Palo Alto, CA 94304

⁴Section on Development and Affective Neuroscience, National Institute of Mental Health Intramural Research Program, 15K North Drive, Bethesda, MD 20892-2670

Keywords

threat learning; adolescent chronic pain; pain catastrophizing; amygdala; hippocampus; vmPFC; fMRI

INTRODUCTION

Neural signals that distinguish threat from safety subserve a fundamental protective mechanism. Acute pain is a survival-relevant threat cue that typically elicits an adaptive neural threat response that diminishes as threat decreases [16]. Yet, when pain becomes chronic, its protective function is lost and the distinction between threat and safety (T-S) becomes imprecise [36]. Dominant biopsychosocial models of chronic pain [56,57] indicate that pain-related distress (catastrophizing and fear) is underpinned by aberrations in T-S discrimination, forming an aberrant affective-learning pathway sustaining pain chronicity [53]. Thus, T-S discrimination has emerged as a treatment target for patients with high pain-related distress, for example via graded in vivo exposure [26,31,54,55,61].

Despite compelling data in adults, there is little understanding of how T-S discrimination confers risk for pain-related distress and chronicity in adolescence. Approximately 1.7 million youth suffer from moderate to severe chronic pain in the US alone [23], conferring risk for continued pain in adulthood [10,27]. In adults, the neural architecture supporting T-S discrimination, hereafter referred to as the 'threat-learning network', involves amygdala,

*Corresponding author: Lauren C. Heathcote (lcheath@stanford.edu). Suite 300, 1070 Arastradero Road, Palo Alto, CA 94304, USA.

CONFLICTS OF INTEREST. Drs. Simons, Borsook, Heathcote, Timmers, Bentley, Youssef, and Pine report no conflicts of interest. Mr./Ms. Kronman, Mahmud, and Hernandez report no conflicts of interest.

hippocampus, insula, anterior cingulate cortex, and ventromedial and dorsolateral prefrontal cortices (vm/dlPFC) [18,19,45]. Amygdala-hippocampus-vmPFC circuitry, in particular, has emerged as core circuitry within the threat-learning network. Converging cross-species evidence outside of pain science shows protracted maturation of threat-learning network circuitry throughout adolescence, potentially implicated in the emergence of pain during this developmental period. Behaviorally, studies show less discrimination between threat and safety cues [29] and attenuated extinction learning [40] in adolescence. At the brain level, adolescents manifest stronger amygdala engagement [29] and altered vmPFC synaptic activity during T-S discrimination, implicated in the formation and regulation of fear responses [40]. Immature prefrontal regulation of subcortical structures during T-S discrimination [40] could create an adolescent vulnerability for pain-related distress and chronicity.

In this study we aimed to elucidate mechanisms of T-S discrimination in adolescent chronic pain patients with high levels of pain-related distress compared to age-matched patients with low distress and healthy controls. We implemented a traditional aversive conditioning approach using a developmentally-appropriate T-S discrimination paradigm [29]. This paradigm includes an acquisition phase (to establish discriminatory learning) and an extinction phase which was completed in the MRI scanner to examine brain responses to the learned threat and safety cues. We investigated activation in individual brain regions within the threat-learning network (region-of-interest analysis) and the interconnected functioning of the network (functional connectivity analysis). We predicted to observe an elevated fear response to a learned threat cue (CS+) in patients with high pain-related distress compared to both patients with low distress and healthy controls, as indexed by 1) elevated self-reported fear and skin conductance response (acquisition and extinction phases), and 2) increased activation in threat-learning network limbic regions (hippocampus, amygdala). We also predicted to observe a deficient safety response (i.e., toward the learned safety cue; CS-) in patients with high pain-related distress, as indexed by 1) elevated self-reported fear and skin conductance response (acquisition and extinction phases), 2) decreased activation in threat-learning network frontal regions (vmPFC, dlPFC), and 3) decreased threat-learning network (fronto-limbic) functional connectivity.

MATERIALS AND METHODS

Participants.

Ninety-seven adolescents were recruited for this study. We adhere to the expanded definition of adolescence as 10–24 years of age [44], reflecting recent consensus regarding continued brain maturation and in line with the population observed at the pediatric pain clinic recruitment site. Six participants were not included in analyses because they terminated the study due to excessive fear ($N = 2$ controls, 1 patient) or no longer met eligibility criteria ($N = 3$ controls). Thus, our final sample included 91 adolescents (78 females): 59 adolescents with chronic pain (defined as pain for >3 months; mean age = 15.5 years) recruited through the Boston Children's Chronic Pain Clinic, and 32 adolescents without chronic pain (mean age = 15.5 years) recruited through local advertisements. The full sample was submitted to self-report and skin conductance analyses to maximize power. Nineteen participants were

not included in the neuroimaging analyses (see exclusions below), thus the final sample submitted to imaging analyses was 72 adolescents. Those participants who were retained in imaging analyses were significantly older ($M = 15.9$ years) than those who were removed ($M = 13.9$ years; $t(89) = -2.9, p = .005$), but did not significantly differ on pain catastrophizing score ($t(89) = 0.79, p = .43$). Participants included in imaging analyses were predominantly white (88.9%).

Adolescent patients reported persistent musculoskeletal, neuropathic, or visceral pain complaints that had persisted for an average of 33.9 months ($SD = 38.6$; Range = 3.4–184.7). Patients reported an average pain intensity of 5.8 out of 10 ($SD = 1.8$; Range = 1–9) and a maximum pain intensity of 8.0 out of 10 ($SD = 1.6$; Range = 2–10) in the preceding four weeks. Patients reported an average pain intensity of 4.1 ($SD = 2.1$, Range = 0–9) at the time of testing. We verified that none of the participants were taking opioid or antipsychotic medications, had significant cognitive impairment, or had significant psychiatric conditions. We did not exclude participants based on comorbid anxiety or depression related to their pain condition, nor on taking selective serotonin reuptake inhibitor (SSRI) medication. This study was approved by the Boston Children's Hospital Institutional Review Board (#P00013786). Participants and legal guardians (for participants <18 years) provided assent/consent.

Self-Report Questionnaires

Demographics and Pain Characteristics.—Participants self-reported age, gender, and pain intensity (10-point Likert scale). Pain duration (months) was calculated from medical records based on when the child's pain started and the study visit date.

Pain Catastrophizing Scale for Children [12].—The PCS-C is a 13-item questionnaire that assesses children's catastrophic thinking about pain, including rumination, magnification, and helplessness. A higher total score indicates greater catastrophizing. The PCS-C has good reliability and validity for young people older than 9 years.

State-Trait Anxiety Inventory for Children [50].—The STAI-C is a 20-item questionnaire that assesses children's state and trait anxiety symptoms via two separate subscales. A higher total score indicates greater anxiety. We used the 10-item Trait subscale as a covariate in analyses to ensure that our findings were specific to pain-related distress rather than more general anxiety symptoms (Pearson correlation between PCS and STAI-C in the current sample: $r = .52, p < .001$; VIF and tolerance indices reveal no issues with multicollinearity).

Functional Disability Inventory [58].—The FDI is a 15-item self-report measure that assesses children's perceived difficulty in performing common activities due to pain. Higher total scores indicate greater disability.

Pain-Related Distress Groupings

We used a median split score on the PCS-C ($Mdn = 22$) to group patients into high and low levels of pain-related distress. We decided *a priori* to divide patients into high and low

distress groupings rather than to examine PCS-C scores continuously (see also [48]). Thus, we aimed to recruit double the number of patients compared to healthy controls to facilitate this grouped design. See Figure 1 for group comparisons on self-report measures.

Experimental Design and Statistical Analysis

Conditioning Paradigm and Study Procedure.—Participants completed an age-appropriate T-S discriminatory task; the ‘Screaming Lady Paradigm’ [8,30] (Figure 2). The task comprises pre-acquisition, acquisition, and extinction phases, presented using Eprime 2.0 software (Psychology Software Tools, Pittsburgh, PA). During pre-acquisition trials ($n = 8$), participants viewed two female actresses displaying neutral facial expressions [52]. During acquisition trials ($n = 20$), after seven seconds the neutral expression of one of the faces (CS+) changed to an intense fear expression for one second that was paired with a 90–95-db scream (US), on 80% of trials. The other face (CS-) remained neutral. During extinction trials ($n = 32$), participants again viewed both actresses displaying only neutral facial expressions. Inter-trial intervals were jittered ranging from 11 to 25 seconds, and trials were separated over two blocks for the extinction phase. The face that served as the CS+, and trial order, were counterbalanced across participants. Due to issues of startle-related movement (from the US) and to prevent participant fatigue, only the extinction phase was completed in the scanner, allowing us to probe neural responses to the learned threat and safety cues. Thus, participants first completed the pre-acquisition and acquisition phases in a separate study room, in the same building as the MRI suite. There was an approximate 30–60-minute break in between acquisition and extinction phases, allowing for completion of post-acquisition measures and relocation to the MRI suite.

Self-Report Ratings Acquisition and Analysis.—Ratings of self-reported anxiousness towards (10-point Likert scale; “not at all anxious” to “extremely anxious”) and perceived unpleasantness (10-point Likert scale; “not at all unpleasant” to “extremely unpleasant”) were collected for each CS by presenting each neutral face on an iPad after each phase. These ratings were combined (mean score) to create a self-reported fear rating. Contingency awareness was assessed after the acquisition phase by asking participants what percentage of the time they thought each CS screamed. While controlling for age and anxiety (centered), F -tests were performed to test interactions between stimulus (CS+, CS-), group (controls, patients low in distress, patients high in distress), and phase (pre-acquisition, acquisition, extinction).

Skin Conductance Response Acquisition and Analysis.—Galvanic skin responses were recorded using Biopac hardware (Biopac Systems, Inc., Goleta, CA, USA), with sensors on the index and middle finger on the non-dominant hand. Skin conductance response (SCR) amplitudes were calculated using the *AcqKnowledge* Event Related Analysis (EDA) tool [4]. This calculates the height of the corresponding SCR as determined by the change in the tonic EDA from the time of SCR onset to the maximum tonic EDA amplitude achieved during the interval from 1s after CS-onset to 6s after CS onset. All raw data was filtered through a high-pass filter at 0.05Hz; additionally, raw data from the extinction phase was filtered through a low-pass filter at 5Hz to filter out MRI-related noise. The first CS+ and CS- trials during pre-acquisition were excluded from analyses to remove

initial orienting effects. Responses below the minimal response criterion (0.01 microsiemens (μS)) were encoded as zero.

For each phase (pre-acquisition, acquisition, and extinction), we analyzed SCRs using Tweedie mixed-effects models (log-link) with fixed effects for stimulus, group, and early versus late sub-phase (50% of trials in each phase; acquisition and extinction only) and participant-level random effects to account for repeated trials. The Tweedie distribution is a special case of an exponential distribution that allows for a cluster of data at zero; thus, it was chosen to appropriately account for the high amount of zero-response SCR data.

Neuroimaging Acquisition and Analysis.—Neuroimaging data were acquired on a 3T MRI scanner (Siemens Magnetom Trio) using a 12-channel head coil. For eight participants, extinction was performed outside of the scanner due to scanner malfunctions ($N=5$) or participant request ($N=3$). Eight participants were excluded due to excessive motion and three participants were excluded due to lack of any vision-related activation in occipital cortex. Thus, 72 participants were included in the final imaging analyses.

For the functional images, a T2*-weighted standard echo-planar imaging (EPI) sequence was used to acquire 51 axial slices (3 mm isotropic) covering the entire cortical volume, using the following parameters: repetition time (TR) = 1110 ms, echo time (TE) = 30 ms, flip angle = 70° , field of view (FOV) = 228×228 mm, matrix size = 76×90 , slice acceleration factor = 3. In total, 430 functional volumes were collected per run. In addition, 8 functional volumes using the same parameters but reverse phase encoding direction (posterior to anterior) were acquired. T1-weighted anatomical images were acquired using a 3D multi-echo magnetization-prepared rapid gradient-echo (ME-MPRAGE) sequence with the following parameters: 176 slices, 1 mm isotropic, TR = 2520 ms, TE1 = 1.74 ms, TE2 3.6 ms, TE3 5.46 ms, TE4 7.32 ms, flip angle = 7° , FOV = 240×240 , GRAPPA acceleration factor = 2.

Pre-processing.: Pre-processing of functional data was initiated with estimation and correction of geometric distortions. From the pairs of EPI images that were acquired using reversed phase-encoding directions (i.e., with distortions facing opposing directions), the susceptibility-induced off-resonance field was estimated using a method similar to the one described in Andersson et al [2] (topup of FMRIB Software Library [FSL] [49]). In a next step, these distortions were corrected in the full functional dataset (FSL applytopup), separate for each run. Pre-processing of the functional data further included 3D rigid motion correction, linear trend removal, co-registration of functional and anatomical data, normalization to MNI space, and spatial smoothing (6 mm FWHM kernel) (using DPARSF [9]).

First-level analyses.: Unless stated otherwise, analysis steps were performed in Statistical Parametric Mapping (SPM12) software [41]. To compare blood-oxygen-level dependent (BOLD) responses to the different stimuli and across groups, a univariate random-effects (RFX) General Linear Model approach was taken using two stages. On the first level, the stimuli (i.e., CS+ and CS-) were modelled as predictors, convolved with the hemodynamic response function (HRF). Individual motion parameters were added to the model as

variables of no interest, including the six motion parameters as well as the first six derivatives of these parameters. In addition, the averaged time course was extracted from the white matter (WM) and cerebrospinal fluid (CSF), and motion outliers were estimated and modeled as stick predictors (FSL's MotionOutliers), and added as nuisance variables. A high-pass filter was applied using a cut-off of 128s. Runs with motion exceeding 6 mm/degrees were excluded from the analysis (i.e., 9 participants were excluded; 7 patients, 1 control). An additional 12 participants (7 patients, 5 controls) had motion between 3 and 6 mm/degrees. In order to be liberal given our pediatric population, we evaluated these runs visually to facilitate decisions to retain or exclude. We contrasted the visual stimuli (CS+, CS-) with baseline and evaluated the quality of the maps visually on an individual level. Three additional participants were excluded based on this procedure (2 patients, 1 control), as they did not show any vision-related activation in occipital cortex. The other participants were retained in the analysis. Following this, comparing mean frame-wise displacement (FD, i.e., within-scan motion; [42]) did not show any significant motion differences across groups ($F(2,69) = 1.23, p = .30$).

Second-level analysis.: The individual contrasts (i.e., CS+ vs. baseline, CS- vs. baseline) were entered into the second level analysis. Controlling for age and anxiety (centered), we performed a $3 \times 2 \times 2$ F -test with group (controls, patients low in distress, patients high in distress) as a between-subject factor, and stimulus (CS+, CS-) and extinction phase (early, late) as within-subject factors. Main effects of stimulus and interactions between group and stimulus were explored at the whole brain level ($p < .001$, cluster extent $k = 10$) to corroborate the selection of our ROIs.

Threat-learning network regions of interest.: For our primary hypotheses, we extracted beta coefficients (estimated activation) from threat-learning network regions of interest (ROIs) using *marsbar* [7]) and analyzed effects of group and stimulus using the same statistical model in SPSS version 25. Our *a priori* ROIs, based on established core threat-learning circuitry described earlier, were the amygdala (basolateral and centromedial), hippocampus, anterior insula (AI), anterior midcingulate cortex (aMCC), and ventromedial and dorsolateral prefrontal cortex (vmPFC, dlPFC). Given their recent emergence as markers of pain chronicity and increasing evidence for involvement in threat-learning mechanisms, we also examined activations in the nucleus accumbens (NAc) [3,60] and periaqueductal gray (PAG) [32]. Regions were extracted as follows: bilateral basolateral and centromedial amygdala (extracted from Julich histological atlas, thresholded at 50%, [1]); bilateral hippocampus, bilateral nucleus accumbens, bilateral ventromedial prefrontal cortex or frontal medial cortex (extracted from Harvard Oxford atlases, thresholded at 50%, [14,17,22,33]); periaqueductal grey (PAG; 10 mm radius sphere around coordinate $x = 4/-4, y = -29, z = 10$, based on Linnman et al [32]); and bilateral anterior insula, bilateral dorsolateral PFC, right anterior mid-cingulate (aMCC) (10 mm radius sphere around peak coordinates from a meta-analysis contrasting CS+>CS- during the extinction phase [18]; left anterior insula $x = -54, y = 8, z = 2$; right anterior insula $x = 28, y = 24, z = -8$, aMCC: $x = 6, y = 38, z = 18$, left dlPFC: $x = -30, y = 46, z = 20$, right dlPFC $x = 34, y = 50, z = 24$).

Functional connectivity analyses.: In addition, a generalized psychophysiological interaction (gPPI) analysis was performed to investigate stimulus-specific changes in functional connectivity across threat-learning network ROIs and potential group differences (using *CONN*; [59]). All ROIs were analyzed as seed regions within each analysis. PPI predictors were created (i.e., interaction term between stimulus and the time course of the seed) as well as two types of confound predictors: psychological predictors (i.e., stimulus predictors, general effect of task) and physiological predictors (i.e., seed time course, as some areas may be correlated with the seed time course regardless of the task). In *CONN*, gPPI is implemented in a similar way as in FSL, convolving the stimulus factors rather than deconvolving the BOLD signal. Main effects of group across both stimuli (i.e., CS+, CS- separately) were evaluated in *CONN* using $p\text{-FDR} < .05$ to account for multiple comparisons, including age and anxiety (centered) as covariates. For significant group effects, betas were extracted and post-hoc comparisons were performed in SPSS version 25.

Associations between Brain, Physiology, and Behaviour.—In order to examine accordance across modalities, and thus whether modalities reflected the same underlying processes, we calculated stimulus difference scores (CS+ > CS-) across all modalities and examined Pearson correlations between self-reported fear, SCR, and extracted beta coefficients in ROIs that yielded significant interactions with group.

RESULTS

Self-Reported Fear

While controlling for age and anxiety, a 2 (stimulus) \times 2 (group) \times 3 (phase) ANOVA yielded main effects of time ($F(2,162) = 10.93, p < .001$) and stimulus ($F(1,81) = 82.88, p < .001$), and an interaction between time and stimulus ($F(2,162) = 45.27, p < .001$) (see Figure 3). These effects were subsumed under a three three-way interaction ($F(4,162) = 2.71, p = .03$), indicating additional differences across groups. As expected, at **pre-acquisition**, there were no significant main effects of group or stimulus, or interaction effects (all $p > .05$). After **acquisition** the 2 (stimulus) \times 3 (group) ANOVA yielded a significant stimulus \times group interaction ($F(2,85) = 5.78, p = .004$). Consistent with successful learning, participants reported significantly higher fear ratings to the CS+ than the CS- in all three groups (all p 's $< .001$). Patients with high pain-related distress reported significantly higher fear ratings to the CS+ compared to both patients with low distress ($p\text{-corrected} = .04$) and controls ($p\text{-corrected} = .04$). Patients low in distress did not significantly differ from controls ($p\text{-corrected} > .05$). After **extinction**, the 2 (stimulus) \times 3 (group) ANOVA again yielded a significant stimulus \times group interaction ($F(2,84) = 6.67, p = .002$). Participants maintained significantly higher fear ratings to the CS+ than the CS- in all three groups (high distress $p < .001$; low distress $p = .03$; controls $p = .048$), indicating some persistence of learned fear. Patients high in distress still reported significantly higher fear to the CS+ compared to controls ($p\text{-corrected} = .01$). Patients low in distress did not significantly differ from patients high in distress or controls ($p\text{-corrected} > .05$).

To further explore the apparent persistence of fear to the CS+ following extinction, a paired-samples t -test revealed a significant difference between fear ratings after acquisition and

after extinction ($t(88) = 3.74, p < .001$; collapsed across groups), with mean fear ratings decreasing across time (acquisition $M = 5.49, SD = 2.21$; extinction $M = 4.56, SD = 2.71$). Thus, findings indicated a significant reduction in learned fear following extinction but not a complete elimination of that fear.

Contingency Awareness

A 2 (stimulus) \times 3 (group) ANOVA yielded a main effect of stimulus only ($F(1,86) = 367.73, p < .001$), reflecting that across all groups, participants were aware that the CS+ ($M = 52.4\%, SD = 25.8$) was paired with the scream more often than the CS- ($M = 0.23\%, SD = 2.62$).

Skin Conductance Response (SCR)

Descriptively, and consistent with learning, a significant difference between stimuli emerged during **acquisition**, reflecting a greater stimulus-evoked SCRs to the CS+ compared to the CS- (Figure 4). This difference was still evident during **extinction**, indicating, like for self-reported fear, a persistent physiological fear response during extinction trials, although the difference was attenuated. Tweedie mixed-effects regression models confirmed that there was no main effect of stimulus at pre-acquisition, again confirming baseline stimulus equivalence. Similarly to the self-report ratings, a main effect of stimulus emerged at **acquisition** and at **extinction** (see Table 1). Tweedie models also confirmed that for both acquisition and extinction, there was a main effect of sub-phase in that SCRs were significantly reduced in the late compared to the early sub-phase. There were no significant differences between groups, and no significant interactions between stimulus and group. Given that no significant two-way interactions emerged, three-way interactions were not tested.

Neural Correlates of T-S Discrimination

Neural activation patterns

Whole brain evoked response.: Whole-brain blood-oxygen-level dependent (BOLD) signal analyses at early extinction confirmed a robust main effect for stimulus in T-S discrimination across participants inclusive and extending beyond the threat-learning network ROIs (Supplementary Figure S1 and Supplementary Table S1). Thus, the whole brain analysis for the interaction between stimulus and group supported the interrogation of our theorized ROIs (Supplementary Figure S2 and Supplementary Table S2). Given substantially less (differential) activation in late extinction compared to early extinction, we describe results separately for early and late extinction sub-phases below.

Threat-learning network during early extinction.: At early extinction, all ROIs yielded a main effect of stimulus or an interaction between stimulus and group. Consistent with successful threat-safety discrimination during the acquisition phase, the left AI, aMCC, PAG, bilateral dlPFC, bilateral centromedial amygdala, and right NAc showed an increased BOLD response to the CS+ compared to the CS- (all p 's $< .05$). There were no interactions with group in these regions (all p 's $> .05$). Significant interactions between stimulus and group were observed in bilateral vmPFC (left: $F(2,67) = 5.63, p = .005$; right: $F(2,67) =$

3.05, $p = .05$), bilateral basolateral amygdala (left: $F(2,67) = 7.81$, $p = .001$; right: $F(2,67) = 6.33$, $p = .003$), bilateral hippocampus (left: $F(2,67) = 8.80$, $p < .001$; right: $F(2,67) = 9.04$, $p < .001$), and left NAc (left: $F(2,67) = 3.66$, $p = .03$; right: $F(2,67) = 1.87$, $p = .16$), indicating differential effects across groups (Figure 5 and explored further below).

For the left and right vmPFC (Figure 5a), patients high in distress showed an increased BOLD response to the CS+ compared to the CS-, while the opposite effect was observed in patients low in distress (i.e., CS- > CS+). Controls showed no significant difference between the CS+ and CS-, however they showed a similar pattern as patients low in distress. Moreover, when comparing groups across stimuli, patients high in distress showed a significantly lower vmPFC BOLD response to the CS- compared to both patients low in distress (left only) and controls; patients low in distress and controls did not significantly differ from each other.

For the hippocampus (Figure 5b) and basolateral amygdala (Figure 5c), patients high in distress showed an increased left-lateralized BOLD response to the CS+ compared to patients low in distress and controls. The right analogues showed a similar pattern. Notably, we also observed opposite differential stimulus effects for patients low in distress versus patients high in distress. That is, while patients low in distress showed significantly increased bilateral BOLD response to the CS- compared to the CS+, patients high in distress showed significantly increased bilateral BOLD response to the CS+ compared to the CS-. Similar to the vmPFC findings, neural activation patterns for bilateral amygdala and hippocampus patients with low distress were aligned with healthy controls.

For the NAc (Figure 5d), there was a significant left-lateralized interaction effect indicating that patients high in distress showed a significantly decreased BOLD response to the CS- compared to both patients low in distress and controls.

Threat-learning network during late extinction. At late extinction, there were significant main effects of stimulus only for the left AI, aMCC, PAG, right dlPFC, and bilateral NA (all p 's $< .05$). These regions all showed a greater response to the CS+ compared to the CS-, indicating an enduring neural threat response in these regions. There were no main effects of group or interactions with group at late extinction.

Post-hoc analyses examining distress (i.e., PCS score) as a continuous variable further supported a priori group comparisons. Specifically, there were significant Pearson correlations between patients' level of distress and differential (CS+>CS-) activation in all ROIs showing an effect of group (all surviving $p < .01$ correction for multiple comparisons). This includes bilateral basolateral amygdala (left: $r = .42$, $p = .005$; right: $r = .47$, $p = .002$), bilateral hippocampus (left: $r = .51$, $p < .001$; right: $r = .47$, $p = .001$), bilateral vmPFC (left: $r = .57$, $p < .001$; right: $r = .52$, $p < .001$), and NAc ($r = .38$, $p = .01$).

Functional Connectivity—Generalized Psychophysiological Interaction (gPPI) analyses was performed to examine group differences in stimulus-specific functional coupling between threat-learning network ROIs. All ROIs were analyzed as seed regions within each analysis. As can be seen in Figure 6, we observed significant group effects for connectivity

between the left vmPFC (seed) and three other regions, specifically in response to the CS-. This included the right hippocampus ($F(2,67) = 5.05$, $p\text{-FDR} = .04$), left centromedial amygdala ($F(2,67) = 6.44$, $p\text{-FDR} = .03$), and right anterior insula ($F(2,67) = 5.83$, $p\text{-FDR} = .03$). There were no significant group differences in response to the CS+. Across all regions, patients high in distress showed significantly greater functional coupling between the vmPFC and all three of these regions in response to the CS- compared to patients low in distress. In addition, patients high in distress also demonstrated significantly greater functional coupling between the vmPFC and the right hippocampus compared to healthy controls. A significant difference between patients low in distress and healthy controls emerged only for the functional coupling between the vmPFC and right anterior insula, for which healthy controls showed greater functional coupling for the CS-.

Associations between Brain, Physiology, and Behaviour

Across the full sample, Pearson correlations revealed a significant positive association between self-reported fear ratings (CS+ > CS-) after acquisition and SCR at early acquisition (Figure 7A). No other associations between SCR and self-report ratings reached significance (all $p > .05$), indicating limited concordance between physiology and behavior apart from initial acquisition. Regarding neural activation patterns, there were significant positive associations between self-reported fear ratings (CS+ > CS-) and differential BOLD activation in a number of threat-learning network regions that previously yielded interactions with group, indicating some concordance between brain activation and behavior. This includes bilateral basolateral amygdala and bilateral hippocampus (Figure 7B). There were no significant associations between SCR and BOLD activation in any ROIs that previously yielded interactions with group.

DISCUSSION

In this study we examined the neural processing of learned threat and safety cues in adolescent chronic pain patients with varying levels of pain-related distress (catastrophizing) as well as healthy controls, using functional MRI. Adolescent patients with high pain-related distress showed elevated self-reported fear and limbic (hippocampus, amygdala) activation in response to a learned threat cue (CS+). They also showed decreased frontal (vmPFC) activation and aberrant fronto-limbic connectivity in response to a learned safety cue (CS-). By comparison, patients with low pain-related distress and healthy controls appeared strikingly similar across brain and behavior. These findings emerged while controlling for age and state anxiety across analyses. A potential mechanistic pathway in chronic pain underlined by differences in T-S discrimination and associated pain-related distress is suggested.

Activations Observed in Threat-Learning Network

Amygdala: Patients with high pain-related distress demonstrated both greater self-reported fear and greater left-lateralized basolateral amygdala activations to the learned threat cue (CS+) compared to healthy controls and compared to patients with low pain-related distress. The amygdala has a well-established role in fear and aversive learning, and our findings are

in line with studies revealing exaggerated amygdala reactivity in individuals with elevated anxiety, including in PTSD populations [6,35,43].

Hippocampus: A similar pattern emerged in the hippocampus, with significantly greater bilateral hippocampal activation for the CS+ in patients with high pain-related distress compared to healthy controls and compared to patients with low pain-related distress. The hippocampus is an important node in corticolimbic circuitry supporting learning and memory [20], particularly in processing contextual fear memories [34]. It is implicated in fear extinction and extinction recall [18] and shows reduced volume and altered connectivity in adult patients with chronic pain [38,39]. It also shows increased activation to threat in anxiety disorders [15], in line with our findings.

vmPFC and its connectivity: While group differences in amygdala and hippocampal activations emerged for the threat cue (CS+), vmPFC differences emerged instead for the safety cue (CS-). Specifically, patients with high pain-related distress showed reduced vmPFC activation for the CS- compared to healthy controls and patients with low pain-related distress. This is in line with prior data revealing attenuated vmPFC activity in anxious individuals [28,46,51]. Moreover, patients with high pain-related distress showed significantly greater functional coupling between the left vmPFC (seed) and right hippocampus, left centromedial amygdala, and right anterior insula in response to the CS- compared to patients with low pain-related distress. This difference was also significant in comparison to controls for the right hippocampus. The vmPFC has received significant attention as critical for the inhibition of fear, potentially due to its role in effortful emotion regulation, although its precise role in fear extinction is still debated [18]. Nonetheless, the mPFC-hippocampus-amygdala circuit is a primary neural substrate of emotional processing and regulation, and is disrupted in anxiety disorders [15]. Our findings provide support for our hypothesis that fronto-limbic connectivity, particularly in the processing of a learned safety cue, is altered in patients with high pain-related distress.

Implications of Observed Brain Activations

We interpret the above findings as follows: (1) Patients with high pain-related distress consistently showed a differential (and opposite) neural response to learned threat and safety cues compared to both healthy controls and patients with low pain-related distress. Thus, differential activation of threat-learning circuitry in adolescents depends on pain-related distress rather than the mere presence of chronic pain. (2) Individual differences in pain-related distress are mediated by fronto-limbic circuitry. Patients with high pain-related distress show a limbically-mediated elevated response to a learned threat cue (CS+), and aberrant fronto-limbic connectivity in response to a learned safety cue (CS-). Thus, group differences in pain-related distress likely reflect a dynamic interplay of regions across the threat-learning network, particularly between the subcortically-driven automatic response to a learned fear and a cortically-driven experience of fear and its effortful inhibition. These findings align with self-report data showing that patients with high pain-related distress reported more fear towards the CS+ compared to both patients with low pain-related distress and healthy controls. Indeed, there were significant correlations between self-reported fear ratings and activation in brain regions of interest across the sample, indicating that cross-

modal findings tap into the same underlying processes. Of note, however, there were no group differences in skin conductance response in either study phase, and no significant correlations between skin conductance and brain activation, potentially indicating a discrepancy with this third modality. (3) Group differences resolved at late extinction. This may reflect an overall habituation effect, or may indicate that pain-related distress is more involved in the initial processing of a previously learned threat cue rather than the subsequent effortful regulation of fear in response to prolonged extinction.

Implications of Threat-Safety Discrimination in Adolescents and Chronic Pain.

Our findings extend a growing literature on T-S discrimination in adolescents. Studies combining multiple psychophysiological measures in developmental populations are rare. Our findings, in one of the largest published samples to date, support using the Screaming Lady task as a reliable experimental measure of aversive learning in young people with chronic health conditions. Previous reports comparing self-reported fear in anxious and non-anxious youth have been mixed, with some studies showing that anxious but not non-anxious youth fail to show differential learning to threat and safety cues, or that non-anxious youth show elevated fear responses [11]. In contrast, our findings concur with studies showing that both anxious and non-anxious children show differential learning to threat and safety cues (indexed by self-report and SCR), but that more anxious youth (here reflected in higher pain-related distress) report greater overall fear toward threat cues [8,30]. Our functional connectivity findings are also in line with other studies examining threat-learning network functioning in adolescents with anxiety disorders, indicating that reduced prefrontal regulation of subcortical structures during T-S discrimination [40] may create an adolescent vulnerability for distress.

Our findings also extend a growing literature on behavioral and neural correlates of pain-related fear. Consistent with a recent meta-analysis by Harvie and colleagues [24], there was no evidence for reduced differential learning between threat and safety stimuli when considering pain patients' self-reported fear. In contrast, both adolescents with and without chronic pain were able to discriminate between threat and safety cues, albeit with an elevated fear response to the threat cue for patients with high pain-related distress. Moreover, although attenuated, this discrimination endured across self-report, SCR, and brain responses even following extinction. These findings mirror previous studies showing that extinction learning is a fragile and often unsuccessful phenomenon [18].

Limitations.

Our study has various limitations including: (1) Sex: Participants were predominantly female, precluding examining sex and gender differences. (2) Age: Participants spanned early adolescence and emerging adulthood (11–24 years). Age was included as a covariate in all primary models; however analyses were underpowered to examine age-related differences. (3) Comorbidity: We excluded participants with significant psychiatric conditions (clinician report) and those taking antipsychotic or opioid medications (child or parent report); however, we did not exclude participants with comorbid depression and anxiety or those taking SSRIs, all of which could influence T-S discrimination. Relatedly, while we controlled for trait anxiety in analyses, it is conceptually erroneous to consider

pain catastrophizing as wholly separable from anxiety. More research attention is needed on the interaction and overlap between pain-specific and generalized anxiety in this population, particularly on their contribution to transdiagnostic processes such as threat learning. (4) *Imaging data for extinction only*: Due to issues of fatigue and startle-related movement (from the scream), only the extinction phase was completed in the scanner. We therefore do not know whether brain-based group differences in the processing of a learned threat are also evident at the initial learning phase; (5) *Task specificity*: It is unclear whether these findings would extend to a pain-specific conditioning task (with a nociceptive US). Our findings point toward a transdiagnostic pathway for pain-related distress that extends beyond learning about pain, to learning more generally about threat. (6) *Causation*: This study indicates that individual differences in T-S discrimination can differentiate patients with high and low pain-related distress, but future studies are needed to clarify whether these aberrations are a cause or consequence of pain-related distress.

Conclusions and Implications for Treatment.

Despite limitations, our findings have implications for chronic pain treatment. Adolescent chronic pain is a risk factor for chronic pain in adulthood [5,25], which costs an estimated \$560 billion each year in direct medical costs, lost productivity, and disability programs in the US alone [21]. Exposure-based therapies that target threat-learning circuitry are now being applied to adolescents with chronic pain [13,47], yet they rely on findings from adult studies where there is mature circuitry and function. Our findings concur with studies demonstrating resistance to extinction in adolescence [40], and could indicate a need to tailor exposure treatments for this developmental group. Recent rodent models reveal that threat conditioning in adolescence accelerates fear behaviors and delays safety expression in adulthood [37]. Thus, delineating how pain-related fear memories formed in adolescence impact adult pain-related learning promises not only to refine exposure-based treatments but also other treatments that utilize extinction principles including psychoeducation, cognitive-behavioral therapy, and biofeedback [24].

Supplementary Material

Refer to Web version on PubMed Central for supplementary material.

Acknowledgments

FUNDING INFORMATION. This study was supported by an R01 grant awarded to Dr. Simons by the National Institutes of Health (#R01HD083270).

REFERENCES

- [1]. Amunts K, Kedo O, Kindler M, Pieperhoff P, Mohlberg H, Shah NJ, Habel U, Schneider F, Zilles K. Cytoarchitectonic mapping of the human amygdala, hippocampal region and entorhinal cortex: Intersubject variability and probability maps. *Anat Embryol (Berl)* 2005;210:343–352. [PubMed: 16208455]
- [2]. Andersson JLR, Skare S, Ashburner J. How to correct susceptibility distortions in spin-echo echo-planar images: Application to diffusion tensor imaging. *Neuroimage* 2003;20:870–888. [PubMed: 14568458]

- [3]. Baliki MN, Petre B, Torbey S, Herrmann KM, Huang L, Schnitzer TJ, Fields HL, Apkarian AV. Corticostriatal functional connectivity predicts transition to chronic back pain. *Nat Neurosci* 2012;15:1117. [PubMed: 22751038]
- [4]. Braithwaite J, Watson D, Robert J, Mickey R. A Guide for Analysing Electrodermal Activity (EDA) & Skin Conductance Responses (SCRs) for Psychological Experiments. *Psychophysiological Res* 2013;49:1017–1034.
- [5]. Brattberg G Do pain problems in young school children persist into early adulthood? A 13-year follow-up. *Eur J Pain* 2004;8:187–199. [PubMed: 15109969]
- [6]. Bremner JD, Staib LH, Kaloupek D, Southwick SM, Soufer R, Charney DS. Neural correlates of exposure to traumatic pictures and sound in Vietnam combat veterans with and without posttraumatic stress disorder: A positron emission tomography study. *Biol Psychiatry* 1999;45:806–816. [PubMed: 10202567]
- [7]. Brett M, Anton JL, Valabregue R, Poline JB. Region of interest analysis using the MarsBar toolbox for SPM99. 8th International Congress on Functional Mapping of the Human Brain. 2002.
- [8]. Britton JC, Grillon C, Lissek S, Norcross MA, Szuhany KL, Chen G, Ernst M, Nelson EE, Leibenluft E, Shechner T, Pine DS. Response to learned threat: An fMRI study in adolescent and adult anxiety. *Am J Psychiatry* 2013;170:1195–1204. [PubMed: 23929092]
- [9]. Chao-Gan Y, Yu-Feng Z. DPARSF: a MATLAB toolbox for “pipeline” data analysis of resting-state fMRI. *Front Syst Neurosci* 2010;4:13. [PubMed: 20577591]
- [10]. Christensen MF, Mortensen O. Long-term prognosis in children with recurrent abdominal pain. *Arch Dis Child* 1975;50:110–114. [PubMed: 1130815]
- [11]. Cohen Kadosh K, Haddad ADM, Heathcote LC, Murphy RA, Pine DS, Lau JYF. High trait anxiety during adolescence interferes with discriminatory context learning. *Neurobiol Learn Mem* 2015;123:50–57. doi:10.1016/j.nlm.2015.05.002. [PubMed: 25982943]
- [12]. Crombez G, Bijttebier P, Eccleston C, Mascagni T, Mertens G, Goubert L, Verstraeten K. The child version of the pain catastrophizing scale (PCS-C): A preliminary validation. *Pain* 2003;104:639–646. [PubMed: 12927636]
- [13]. Dekker C, Goossens MEJB, Bastiaenen CHG, Verbunt JAMCF. Study protocol for a multicentre randomized controlled trial on effectiveness of an outpatient multimodal rehabilitation program for adolescents with chronic musculoskeletal pain (2B Active). *BMC Musculoskelet Disord* 2016;17:317. [PubMed: 27464953]
- [14]. Desikan RS, Ségonne F, Fischl B, Quinn BT, Dickerson BC, Blacker D, Buckner RL, Dale AM, Maguire RP, Hyman BT, Albert MS, Killiany RJ. An automated labeling system for subdividing the human cerebral cortex on MRI scans into gyral based regions of interest. *Neuroimage* 2006;31:968–980. [PubMed: 16530430]
- [15]. Duval ER, Javanbakht A, Liberzon I. Neural circuits in anxiety and stress disorders: A focused review. *Ther Clin Risk Manag* 2015;11:115. [PubMed: 25670901]
- [16]. Elman I, Borsook D. Threat response system: Parallel brain processes in pain vis-à-vis fear and anxiety. *Front Psychiatry* 2018;9:29. [PubMed: 29515465]
- [17]. Frazier JA, Chiu S, Breeze JL, Makris N, Lange N, Kennedy DN, Herbert MR, Bent EK, Koneru VK, Dieterich ME, Hodge SM, Rauch SL, Grant PE, Cohen BM, Seidman LJ, Caviness VS, Biederman J. Structural brain magnetic resonance imaging of limbic and thalamic volumes in pediatric bipolar disorder. *Am J Psychiatry* 2005;162:1256–1265. [PubMed: 15994707]
- [18]. Fullana MA, Albajes-Eizaguirre A, Soriano-Mas C, Vervliet B, Cardoner N, Benet O, Radua J, Harrison BJ. Fear extinction in the human brain: A meta-analysis of fMRI studies in healthy participants. *Neurosci Biobehav Rev* 2018;88:16–25. [PubMed: 29530516]
- [19]. Fullana MA, Harrison BJ, Soriano-Mas C, Vervliet B, Cardoner N, Àvila-Parcet A, Radua J. Neural signatures of human fear conditioning: An updated and extended meta-analysis of fMRI studies. *Mol Psychiatry* 2016;4:500.
- [20]. Ganella DE, Barendse MEA, Kim JH, Whittle S. Prefrontal-Amygdala Connectivity and State Anxiety during Fear Extinction Recall in Adolescents. *Front Hum Neurosci* 2017;11:587. [PubMed: 29255411]

- [21]. Gaskin DJ, Richard P. The economic costs of pain in the United States. *J Pain* 2012;13:715–724. [PubMed: 22607834]
- [22]. Goldstein JM, Seidman LJ, Makris N, Ahern T, O'Brien LM, Caviness VS, Kennedy DN, Faraone SV., Tsuang MT. Hypothalamic Abnormalities in Schizophrenia: Sex Effects and Genetic Vulnerability. *Biol Psychiatry* 2007;61:935–945. [PubMed: 17046727]
- [23]. Groenewald CB, Essner BS, Wright D, Fesinmeyer MD, Palermo TM. The economic costs of chronic pain among a cohort of treatment seeking adolescents in the United States. *J Pain* 2014;15:925–933. doi:10.1016/j.jpain.2014.06.002. [PubMed: 24953887]
- [24]. Harvie DS, Moseley GL, Hillier SL, Meulders A. Classical Conditioning Differences Associated With Chronic Pain: A Systematic Review. *J Pain* 2017;18:889–898. [PubMed: 28385510]
- [25]. Hestbaek L, Leboeuf-Yde C, Kyvik KO, Manniche C. The course of low back pain from adolescence to adulthood: Eight-year follow-up of 9600 twins. *Spine (Phila Pa 1976)* 2006;31:468–472. [PubMed: 16481960]
- [26]. Den Hollander M, Goossens M, De Jong J, Ruijgrok J, Oosterhof J, Onghena P, Smeets R, Vlaeyen JWS. Expose or protect? A randomized controlled trial of exposure in vivo vs pain-contingent treatment as usual in patients with complex regional pain syndrome type 1. *Pain* 2016.
- [27]. Kashikar-Zuck S, Parkins IS, Ting TV., Verkamp E, Lynch-Jordan A, Passo M, Graham TB. Controlled follow-up study of physical and psychosocial functioning of adolescents with juvenile primary fibromyalgia syndrome. *Rheumatology* 2010.
- [28]. Kim MJ, Gee DG, Loucks RA, Davis FC, Whalen PJ. Anxiety Dissociates dorsal and ventral medial prefrontal cortex functional connectivity with the amygdala at rest. *Cereb Cortex* 2011;21:1667–1673. [PubMed: 21127016]
- [29]. Lau JY, Britton JC, Nelson EE, Angold A, Ernst M, Goldwin M, Grillon C, Leibenluft E, Lissek S, Norcross M, Shiffrin N, Pine DS. Distinct neural signatures of threat learning in adolescents and adults. *Proc Natl Acad Sci* 2011;108:4500–4505. [PubMed: 21368210]
- [30]. Lau JYF, Lissek S, Nelson EE, Lee Y, Roberson-Nay R, Poeth K, Jenness J, Ernst M, Grillon C, Pine DS. Fear conditioning in adolescents with anxiety disorders: Results from a novel experimental paradigm. *J Am Acad Child Adolesc Psychiatry* 2008;47:94–102. [PubMed: 18174830]
- [31]. Leeuw M, Goossens MEJB, van Breukelen GJP, de Jong JR, Heuts PHTG, Smeets RJEM, Köke AJA, Vlaeyen JWS. Exposure in vivo versus operant graded activity in chronic low back pain patients: Results of a randomized controlled trial. *Pain* 2008.
- [32]. Linnman C, Moulton EA, Barmettler G, Becerra L, Borsook D. Neuroimaging of the periaqueductal gray: State of the field. *Neuroimage* 2012;60:505–522. [PubMed: 22197740]
- [33]. Makris N, Goldstein JM, Kennedy D, Hodge SM, Caviness VS, Faraone SV., Tsuang MT, Seidman LJ. Decreased volume of left and total anterior insular lobule in schizophrenia. *Schizophr Res* 2006;83:155–171. [PubMed: 16448806]
- [34]. Maren S, Phan KL, Liberzon I. The contextual brain: Implications for fear conditioning, extinction and psychopathology. *Nat Rev Neurosci* 2013;14:417. [PubMed: 23635870]
- [35]. Milad MR, Pitman RK, Ellis CB, Gold AL, Shin LM, Lasko NB, Zeidan MA, Handwerker K, Orr SP, Rauch SL. Neurobiological Basis of Failure to Recall Extinction Memory in Posttraumatic Stress Disorder. *Biol Psychiatry* 2009;66:1075–1082. [PubMed: 19748076]
- [36]. Moseley GL, Vlaeyen JWS. Beyond nociception: the imprecision hypothesis of chronic pain. *Pain* 2015;156.
- [37]. Müller I, Brinkman AL, Sowinski EM, Sangha S. Adolescent conditioning affects rate of adult fear, safety and reward learning during discriminative conditioning. *Sci Rep* 2018;8:17315. doi: 10.1038/s41598-018-35678-9. [PubMed: 30470766]
- [38]. Mutso AA, Petre B, Huang L, Baliki MN, Torbey S, Herrmann KM, Schnitzer TJ, Apkarian AV. Reorganization of hippocampal functional connectivity with transition to chronic back pain. *J Neurophysiol* 2014;111:1065–1076. [PubMed: 24335219]
- [39]. Mutso AA, Radzicki D, Baliki MN, Huang L, Banisadr G, Centeno MV., Radulovic J, Martina M, Miller RJ, Apkarian AV. Abnormalities in Hippocampal Functioning with Persistent Pain. *J Neurosci* 2012;32:5747–5756. [PubMed: 22539837]

- [40]. Pattwell SS, Duhoux S, Hartley CA, Johnson DC, Jing D, Elliott MD, Ruberry EJ, Powers A, Mehta N, Yang RR, Soliman F, Glatt CE, Casey BJ, Ninan I, Lee FS. Altered fear learning across development in both mouse and human. *Proc Natl Acad Sci* 2012;109:6318–16323.
- [41]. Penny W, Friston K, Ashburner J, Kiebel S, Nichols T. *Statistical Parametric Mapping: The Analysis of Functional Brain Images*. 2007 p.
- [42]. Power JD, Barnes KA, Snyder AZ, Schlaggar BL, Petersen SE. Spurious but systematic correlations in functional connectivity MRI networks arise from subject motion. *Neuroimage* 2012.
- [43]. Rauch SL, Shin LM, Phelps EA. Neurocircuitry Models of Posttraumatic Stress Disorder and Extinction: Human Neuroimaging Research-Past, Present, and Future. *Biol Psychiatry* 2006;60:376–382. [PubMed: 16919525]
- [44]. Sawyer SM, Azzopardi PS, Wickremarathne D, Patton GC. The age of adolescence. *Lancet Child Adolesc Heal* 2018;2:223–228.
- [45]. Sehlmeier C, Schöning S, Zwitserlood P, Pfliegerer B, Kircher T, Arolt V, Konrad C. Human fear conditioning and extinction in neuroimaging: A systematic review. *PLoS One* 2009;6:5865.
- [46]. Simmons A, Matthews SC, Feinstein JS, Hitchcock C, Paulus MP, Stein MB. Anxiety vulnerability is associated with altered anterior cingulate response to an affective appraisal task. *Neuroreport* 2008;19:1033–1037. [PubMed: 18580574]
- [47]. Simons LE. GET Living: Graded Exposure Treatment for Children and Adolescents With Chronic Pain. 2018 n.d. Available: <https://clinicaltrials.gov/ct2/show/NCT03699007>.
- [48]. Simons LE, Erpelding N, Hernandez JM, Serrano P, Zhang K, Lebel AA, Sethna NF, Berde CB, Prabhu SP, Becerra L, Borsook D. Fear and Reward Circuit Alterations in Pediatric CRPS. *Front Hum Neurosci* 2016;9:703. [PubMed: 26834606]
- [49]. Smith SM, Jenkinson M, Woolrich MW, Beckmann CF, Behrens TEJ, Johansen-Berg H, Bannister PR, De Luca M, Drobnjak I, Flitney DE, Niazy RK, Saunders J, Vickers J, Zhang Y, De Stefano N, Brady JM, Matthews PM. Advances in functional and structural MR image analysis and implementation as FSL. *Neuroimage* 2004;23:S208–S219. [PubMed: 15501092]
- [50]. Spielberger CD, Edwards CD, Lushene RE, Montuori J, Platzek D. *The State-Trait Anxiety Inventory for Children (preliminary manual)*. Palo Alto, CA: Consulting Psychologists Press, 1973 p.
- [51]. Straube T, Schmidt S, Weiss T, Mentzel HJ, Miltner WHR. Dynamic activation of the anterior cingulate cortex during anticipatory anxiety. *Neuroimage* 2009;44:975–981. [PubMed: 19027072]
- [52]. Tottenham N, Tanaka JW, Leon AC, McCarry T, Nurse M, Hare TA, Marcus DJ, Westerlund A, Casey BJ, Nelson C. The NimStim set of facial expressions: Judgments from untrained research participants. *Psychiatry Res* 2009;168:242–249. [PubMed: 19564050]
- [53]. Vlaeyen JWS, Crombez G, Linton SJ. The fear-avoidance model of pain. *Pain* 2016;157:1588–1589. [PubMed: 27428892]
- [54]. Vlaeyen JWS, De Jong J, Geilen M, Heuts PHTG, Van Breukelen G. Graded exposure in vivo in the treatment of pain-related fear: A replicated single-case experimental design in four patients with chronic low back pain. *Behav Res Ther* 2001.
- [55]. Vlaeyen JWS, De Jong J, Geilen M, Heuts PHTG, Van Breukelen G. The treatment of fear of movement/(re)injury in chronic low back pain: Further evidence on the effectiveness of exposure in vivo. *Clin J Pain* 2002.
- [56]. Vlaeyen JWS, Linton SJ. Fear-avoidance and its consequences in chronic musculoskeletal pain: A state of the art. *Pain* 2000;85:317–332. [PubMed: 10781906]
- [57]. Vlaeyen JWS, Linton SJ. Fear-avoidance model of chronic musculoskeletal pain: 12 years on. *Pain* 2012;153:1144–1147. [PubMed: 22321917]
- [58]. Walker LS, Greene JW. The functional disability inventory: measuring a neglected dimension of child health status. *J Pediatr Psychol* 1991;16:39–58. [PubMed: 1826329]
- [59]. Whitfield-Gabrieli S, Nieto-Castanon A. Conn: A Functional Connectivity Toolbox for Correlated and Anticorrelated Brain Networks. *Brain Connect* 2012;2:125–141. [PubMed: 22642651]

- [60]. Woo CW, Roy M, Buhle JT, Wager TD. Distinct Brain Systems Mediate the Effects of Nociceptive Input and Self-Regulation on Pain. *PLoS Biol* 2015;13:e1002036. [PubMed: 25562688]
- [61]. Woods MP, Asmundson GJG. Evaluating the efficacy of graded in vivo exposure for the treatment of fear in patients with chronic back pain: A randomized controlled clinical trial. *Pain* 2008.

Author Manuscript

Author Manuscript

Author Manuscript

Author Manuscript

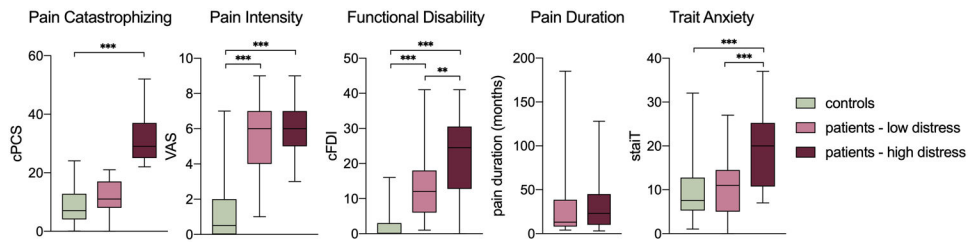


Figure 1. Psychological and pain profiles across groups. * $p < .05$, ** $p < .01$, *** $p < .001$. All p values Bonferroni corrected. Note: Multiple comparisons for PCS-C scores were not examined between patient groups to avoid circular analyses given that this measure was used to create groupings.

Author Manuscript

Author Manuscript

Author Manuscript

Author Manuscript

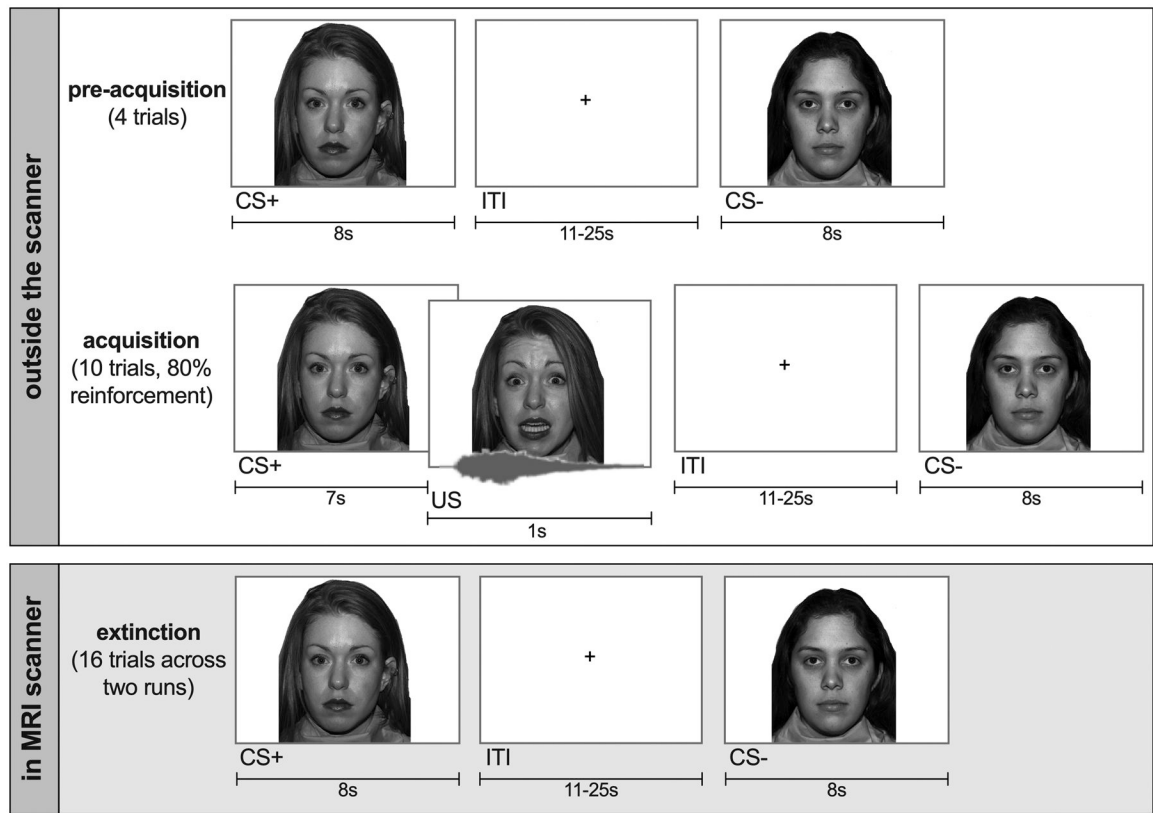


Figure 2.
Screaming Lady Paradigm.

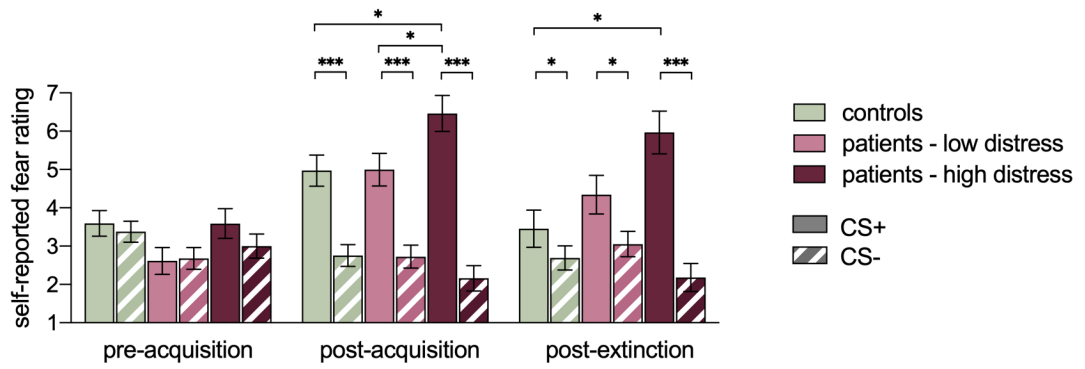


Figure 3. Self-reported fear ratings to the CS+ and CS- across groups and study phases. Significance values reflect decomposed simple effects following a significant three-way interaction. Main effects of group or stimulus not depicted for visual simplicity. * $p < .05$, *** $p < .001$. All p values Bonferroni corrected.

Author Manuscript

Author Manuscript

Author Manuscript

Author Manuscript

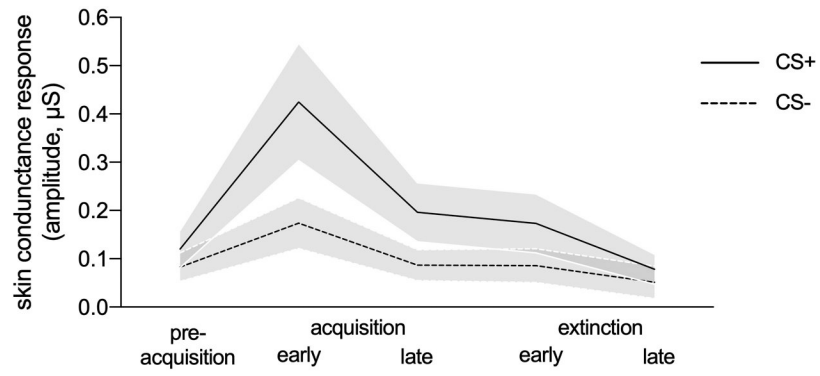


Figure 4. Skin conductance response (SCR) amplitudes for the CS+ and CS- collapsed across all participants, averaged across study phases, and early and late extinction sub-phases.

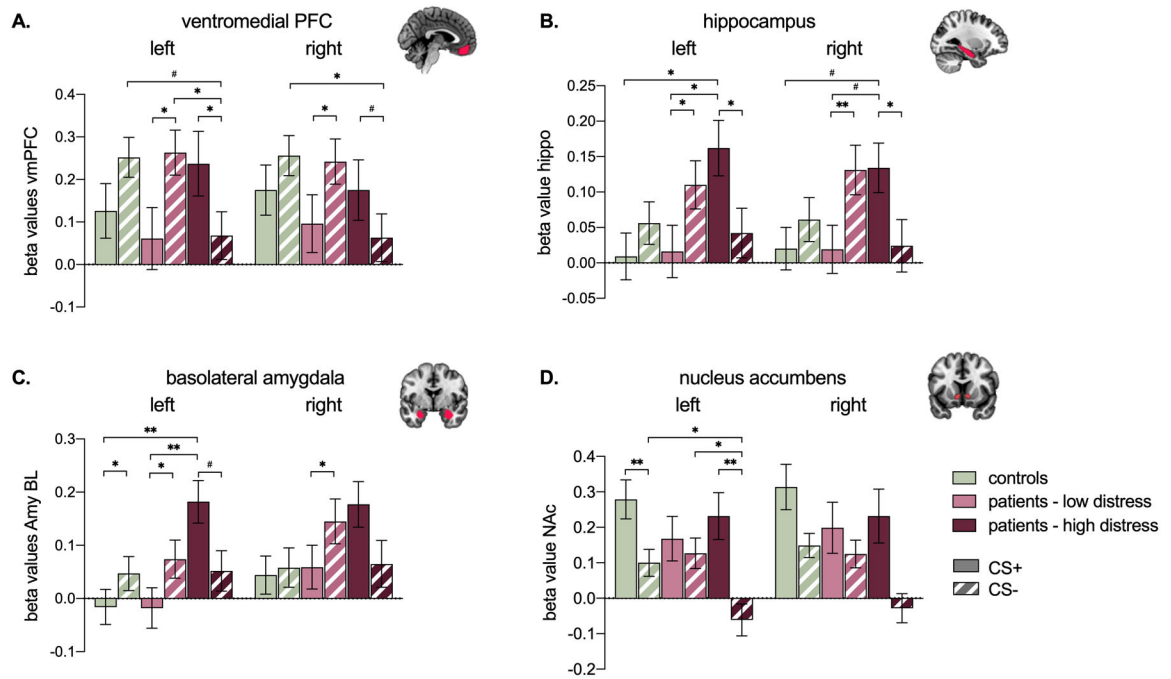


Figure 5. Beta coefficients reflecting BOLD responses to the CS+ and CS- at early extinction, across groups. # $p < .08$, * $p < .05$, ** $p < .01$. All p values Bonferroni corrected. Main effects of group or stimulus not depicted for visual simplicity.

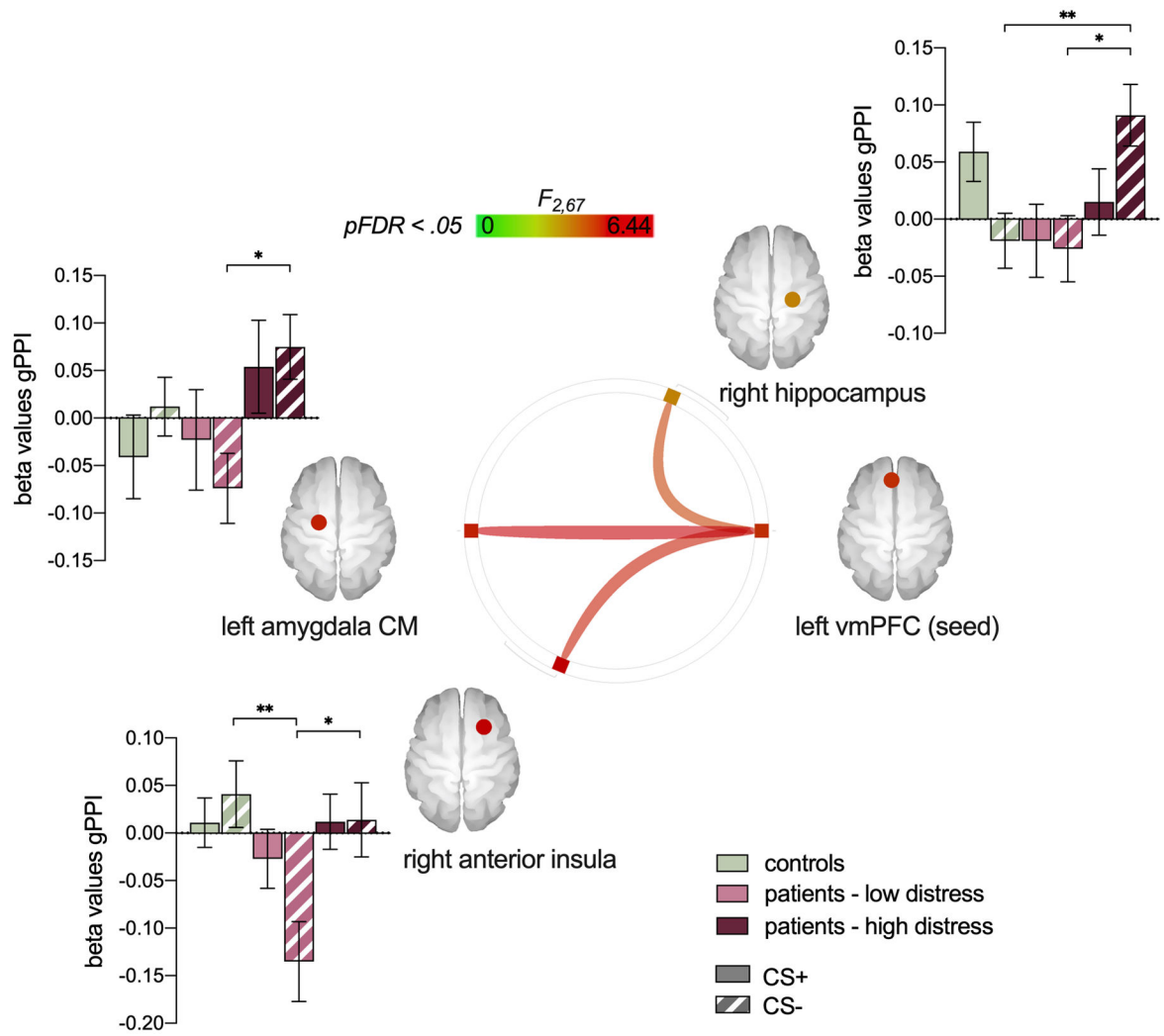


Figure 6. Beta coefficients reflecting condition-specific functional connectivity across ROIs. * $p < .05$, ** $p < .01$. All p values Bonferroni corrected.

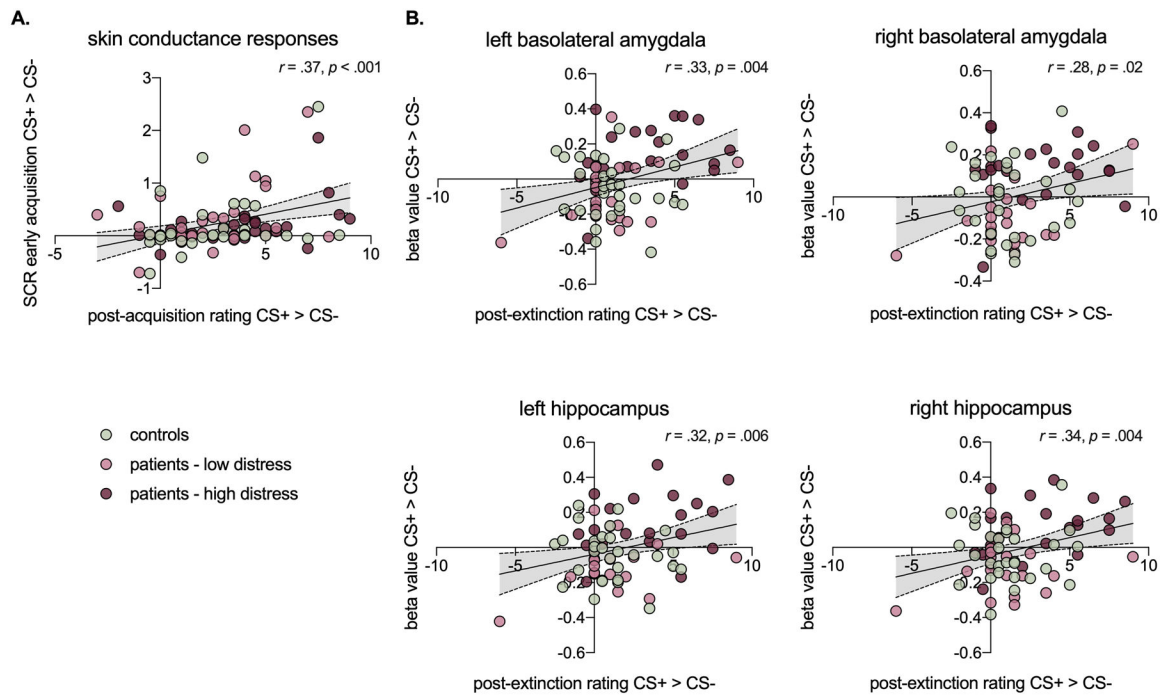


Figure 7. Scatterplots showing significant cross-modality Pearson correlations

TABLE 1. Adjusted associations for stimulus, group, and sub-phase period with mean skin conductance response*

Stimulus	Pre-acquisition			Acquisition			Extinction		
	Number of trials (participants)	β (95% CI) ¹	P-value ²	Number of trials (participants)	β (95% CI) ¹	P-value ²	Number of trials (participants)	β (95% CI) ¹	P-value ²
CS-	528 (88)	0 (reference)	.07	1778 (89)	0 (reference)	< .001	2547 (80)	0 (reference)	< .001
CS+		0.45 (-0.02, 0.93)			0.77 (0.54, 1.00)			0.63 (0.39, 0.86)	
Group			.36			.64			.64
Control		0 (reference)			0 (reference)			0 (reference)	
Patients (Low)		0.62 (-0.26, 1.50)			-0.03 (-0.76, 0.71)			0.37 (-0.63, 1.42)	
Patients (High)		0.55 (-0.34, 1.43)			0.30 (-0.42, 1.02)			0.48 (-0.54, 1.51)	
Sub-phase period			n/a			< .001			< .001
Early		n/a			0 (reference)			0 (reference)	
Late		n/a			-0.81 (-1.04, -0.57)			-0.68 (-0.92, -0.45)	

* Tweedie mixed-effects regression models fit using maximum likelihood and a log-link via the cplm package available in R assuming missing at random. Mean skin conductance response values truncated at the 99.5th percentile within study phase to mitigate effects of outliers.

¹ Regression coefficients are for a change on log mean and can be exponentiated to determine the multiplicative effect on the original scale (i.e., $\exp(0.45) = 1.57$).

² P-value for likelihood ratio test.